



## Obrabotka metallov -

# Metal Working and Material Science

Journal homepage: [http://journals.nstu.ru/obrabotka\\_metallov](http://journals.nstu.ru/obrabotka_metallov)



## Investigation on the electrical discharge machining of cryogenic treated beryllium copper (BeCu) alloys

Dhruv Sawant<sup>1, a</sup>, Rujuta Bulakh<sup>1, b</sup>, Vijaykumar Jatti<sup>1, c, \*</sup>, Satish Chinchani<sup>2, d</sup>,  
 Akshansh Mishra<sup>3, e</sup>, Eyob Messele Sefene<sup>4, 5, f</sup>

<sup>1</sup> Symbiosis Institute of Technology, Pune-412115, Maharashtra State, India

<sup>2</sup> Vishwakarma Institute of Information Technology, Kondhwa (Budruk), Pune - 411039, Maharashtra, India

<sup>3</sup> School of Industrial and Information Engineering, Politecnico Di Milano, 22 Leonardo str., Milan, Italy

<sup>4</sup> National Taiwan University of Science and Technology, 43 Keelung Rd., Taipei, 106335, Taiwan

<sup>5</sup> Bahir Dar Institute of Technology, Bahir Dar, Amhara, Ethiopia

<sup>a</sup>  <https://orcid.org/0009-0009-9543-690X>,  [dhruv.sawant.btech2022@sitpune.edu.in](mailto:dhruv.sawant.btech2022@sitpune.edu.in);

<sup>b</sup>  <https://orcid.org/0009-0000-4594-3385>,  [rujuta.bulakh.btech2022@sitpune.edu.in](mailto:rujuta.bulakh.btech2022@sitpune.edu.in);

<sup>c</sup>  <https://orcid.org/0000-0001-7949-2551>,  [vijaykumar.jatti@sitpune.edu.in](mailto:vijaykumar.jatti@sitpune.edu.in);

<sup>d</sup>  <https://orcid.org/0000-0002-4175-3098>,  [satish.chinchani@viit.ac.in](mailto:satish.chinchani@viit.ac.in);

<sup>e</sup>  <https://orcid.org/0000-0003-4939-359X>,  [akshansh.mishra@mail.polimi.it](mailto:akshansh.mishra@mail.polimi.it);

<sup>f</sup>  <https://orcid.org/0000-0003-4660-6262>,  [eyobsmart27@gmail.com](mailto:eyobsmart27@gmail.com)

### ARTICLE INFO

#### Article history:

Received: 18 November 2023

Revised: 08 January 2024

Accepted: 22 January 2024

Available online: 15 March 2024

#### Keywords:

Beryllium copper

Cryogenic treatment

Material removal rate

White layer thickness

Surface crack formation

### ABSTRACT

**Introduction.** In modern manufacturing world, industries should adapt technological advancements for precision machining of difficult-to-machine metals, especially for beryllium copper (*BeCu*) alloys. The electrical discharge machining of alloys has proven its viability. **The purpose of the work.** A literature review indicated that the investigation of electrical discharge machining of *BeCu* alloys is still in its infancy. Furthermore, the cryogenic treatment of workpieces and electrodes in electrical discharge machining has not received much attention from researchers. Moreover, the impact of magnetic field strength on surface integrity and productivity during electrical discharge machining has not attracted much attention from researchers. **The methods of investigation.** This paper describes the use of electrolytic copper with different gap current values, pulse on periods, and external magnetic strength for electrical discharge machining of *BeCu* alloys. This paper examines how the material removal rate, the thickness of the white layer, and the formation of surface cracks are affected by cryogenic treatment of the workpiece and tool, pulse-on time, gap current, and magnetic strength. **Results and Discussion.** The combination of the cryogenically treated *BeCu* workpiece and the untreated *Cu* electrode had the highest material removal rate among all the combinations of workpieces and tools used in this study. The pulse on-time and the strength of the magnetic field had little influence on material removal rate, whereas the gap current had the greatest effect. The maximum achieved material removal rate was 11.807 mm<sup>3</sup>/min. At a high material removal rate, the observed thickness of the white layer on the horizontal surface ranged from 12.92 μm to 14.24 μm. In the same way, the maximum and minimum values for the vertical surface were determined to be 15.58 μm and 11.67 μm, respectively. According to scanning electron microscopy, the layer thickness was less than 20 μm, and barely noticeable surface cracks were observed in specimens with low, medium and high material removal rates. Obviously, due to the cryogenic processing of the workpiece and the external magnetic strength, there was a slight cracking of the surface and the formation of a white layer.

**For citation:** Sawant D., Bulakh R., Jatti V., Chinchani S., Mishra A., Sefene E.M. Investigation on the electrical discharge machining of cryogenic treated beryllium copper (BeCu) alloys. *Obrabotka metallov (tehnologiya, oborudovanie, instrumenty) = Metal Working and Material Science*, 2024, vol. 26, no. 1, pp. 175–193. DOI: 10.17212/1994-6309-2024-26.1-175-193. (In Russian).

#### \* Corresponding author

Jatti Vijaykumar S., Ph.D. (Engineering), Professor

Symbiosis Institute of Technology,

Pune – 412115, Maharashtra State, India

Tel.: 91-2028116300, e-mail: [vijaykumar.jatti@sitpune.edu.in](mailto:vijaykumar.jatti@sitpune.edu.in)

## Introduction

*BeCu* alloys, or beryllium copper alloys, are very reliable materials with outstanding fatigue strength, hardness, wear resistance, and non-magnetic characteristics that are utilized in a variety of industries. A consistent, homogeneous liquid solution is obtained by combining beryllium and copper, which is a distinctive feature of the microstructure. Copper frequently retains its face-centered cubic form, and beryllium becomes a crucial part of the copper crystal. When copper atoms are replaced by beryllium atoms in the same lattice regions, a substitutional solid solution is produced. *BeCu* alloys have been used to create breaker reeds, diaphragms, control valves, switchgear components, and all varieties of flat and coil springs. High electrical conductivity and toughness have also been used in plastic extrusion dies and specialty tooling. However, there are several problems when utilizing traditional machining methods to cut *BeCu* alloys. Due to the high strength of *BeCu* alloys, it is problematic to maintain the integrity of the surface of the finished product, and increased tool wear occurs during machining. *BeCu* alloys have good thermal and electrical properties, which make electrical discharge machining safe and effective.

For cutting hard materials, electrical discharge machining (*EDM*) is a practical technique [1–6]. Due to the complexity of the process, numerous studies on electrical discharge machining have been conducted to determine its' optimal parameters [7–10]. The main objective of this research is to develop a production system that improves material removal rate (*MRR*). Using machine learning (*ML*) techniques, a group of researchers created performance prediction models for *EDM*, including *MRR* [11–13].

*EDM* process modeling development was discussed in detail by *Ming et al.* [14]. *Shastri et al.* [15] assessed the effects of cooling, ultrasonic machining, powder mixture machining, and cryogenic machining on performance indicators such *MRR*, tool wear rate (*TWR*), surface integrity, and recast layer. *Boopathi* [16] offered a comprehensive analysis of the literature on different dielectric fluids, previously unknown and sustainable innovations, process parameters, machining characteristics, and optimization strategies used in various dry and near-dry *EDMs*. The purpose of combining dry and near-dry *EDM* research was to support environmentally friendly *EDM* research projects. The impact of *EDM* die sinking settings on the *MRR* of *BeCu* alloys was examined by *Ali et al.* [17].

The effects of *EDM* settings on the *MRR*, tool wear, relative electrode wear, and surface roughness of *NiTi* alloys were examined by *Daneshmand et al.* [18]. The voltage, discharge current, pulse-on time, and pulse-off time are some of these parameters. The tests were designed using the *L18* orthogonal matrix using the *Taguchi* methodology. The effects of current, voltage, tool rotation,  $Al_2O_3$  powder, *MRR*, *TWR*, and surface roughness were examined by *Daneshmand et al.* [19]. The results show that the *MRR* can be increased by using  $Al_2O_3$  powder, rotating the tool, and raising the voltage, current strength, and pulse width. The effects of electrical discharge machining on the environment, human health, and safety were examined by *Baroi et al.* [20]. The effects of cryogenic treatment on *Inconel 718* work material were investigated by *Kannan et al.* [21]. The cooling effect of copper electrodes during the electrical discharge die sinking of a titanium alloy (*Ti-6Al-4V*) was investigated by *Abdulkareem et al.* [22]. The effects of cooling on workpiece surface roughness and electrode wear have been studied. In order to find out how the *Ti 6246* alloy's machinability was influenced by deep cryogenic treatment, *Gill and Singh* [23] used an electrolytic copper tool to drill blind holes 10 mm in diameter. Furthermore, a comparison was conducted between the untreated *Ti 6246* alloy and the deep cryogenically treated *Ti 6246* alloy in terms of surface roughness and overcut of holes. Copper electrode cooling during electrical discharge machining (*EDM*) of a workpiece composed of *M2*-grade high-speed steel was investigated by *Srivastava and Pandey* [24]. Machinability was evaluated using electrode wear ratio (*EWR*) and surface roughness (*SR*). A study by *Yildiz et al.* [25] investigated the effect of cryogenic and cold processing on the *EDM* machinability of *BeCu* alloy workpieces. The *BeCu* alloy was treated at temperatures of about  $-150^{\circ}F$  ( $-100^{\circ}C$ ) for cold treatment and  $-300^{\circ}F$  ( $-185^{\circ}C$ ) for cryogenic treatment in this investigation.

The titanium *EDM* machining properties were studied by *Singh and Singh* [26] both before and after the tool and workpiece were cryogenically treated. The study's output metrics included dimensional accuracy, surface roughness, *TWR*, and *MRR*. Copper's thermal conductivity was greatly enhanced by

cryogenic treatment in an experimental study conducted by *Nadig et al.* [27]. The thermal conductivity was only marginally enhanced by tempering as compared to cryogenic treatment. The results pave the way for further research to optimize temperature and duration of cryogenic treatment as well as other tempering parameters. During the *EDM* of high-speed steel *M2*, *Srivastava* and *Pandey* [28] assessed surface roughness (*SR*), material removal rate (*MRR*), and electrode wear ratio (*EWR*) using an ultrasonic-assisted cryogenically cooled copper electrode. The discharge current, duty cycle, gap voltage, and pulse-on time were the variables that could be adjusted during the process. In the electrical discharge machining process, three types of electrodes were compared: conventional, cryogenically cooled, and cryogenically cooled together with ultrasound. The *MRR*, *EWR*, and *SR* were measured. The reattachment of particles to the machined surface caused major difficulties in dry *EDM*, according to *Liqing* and *Yingjie* [29]. Their research proposed two methods for increasing *MRR* in dry *EDM*: the first involves the use of cryogenically cooled workpieces, and the second involves the use of dry *EDM* in combination with oxygen gas. Electrical resistivity, crystallite size, microhardness, and microscopic studies were provided by *Jafferson* and *Hariharan* [30], and a comparison of the machining performance of cryogenically treated and untreated microelectrodes in *MEDM* was carried out. The effect of cryogenically treated tool electrodes on electrical discharge machining (*EDM*) processes was studied by *Mathai et al.* [31]. When machining is performed using electrodes subjected to cryogenic treatment of varying durations, the efficiency of the process is examined by examining the change in critical response characteristics, such as *MRR*, *TWR*, and surface roughness, with respect to current and pulse-on time.

The study conducted by *Singh et al.* [32] aimed to evaluate the effectiveness of the copper electrode manufactured through a novel fast manufacturing process in *EDM* on *D-2* steel. On the other hand, *Prakash et al.* [33] focused on comparing the performance of untreated and cryogenically treated micro-*EDM* tool electrodes while machining the magnesium alloy *AZ31B*. The tool electrodes were subjected to cryogenic treatment to enhance its mechanical characteristics, such as hardness and wear resistance, which in turn improved the quality of the machined features. A group of researchers optimized the process parameters using multi-criteria decision-making (*MCDM*) during the *EDM* of *AA6061-T6 SiC* composites (15 wt. % *SiC*) [34]. Attempts were made using supervised machine learning to predict the *EDM* surface roughness of deep cryogenically treated *NiTi*, *NiCu* and *BeCu* alloys [35]. [35].

A review of the literature showed that the research on electrical discharge machining of *BeCu* alloys is still in its infancy. Furthermore, the cryogenic treatment of workpieces and electrodes in *EDM* has not received much attention from researchers. Moreover, the impact of magnetic field strength on surface integrity and productivity during *EDM* has received very little attention in research. Therefore, the goal of this study is to ascertain how the material removal rate, thickness of the white layer, and creation of surface cracks are affected by a cryogenically treated workpiece and electrode, magnetic strength, gap current, and pulse on time. In addition, this study makes use of machine learning regression algorithms to estimate the *MRR*. The remainder of the work consists of sections devoted to materials and methods, results and their discussion, as well as conclusions.

## Materials and Design

In this study, an *Electronica Machine Tools Limited* die sink-type electrical discharge machine, model *C400x250*, was used for testing. A block of 100×100×50 mm in size was used as a workpiece in this study, which was then divided into blocks of 30×20×20 mm in size for carrying out experiments. Copper with high thermal conductivity was used as the tool electrode material in the experiments. The tool had a square shape with dimensions of 6×90 mm, respectively. Using an indexing system and a milling machine, it was given a 3×25 mm square shape.

During the experiment, an external magnetic field was applied using a neodymium magnet surrounding the cutting zone. The workpiece and tool electrodes were cryogenically prepared prior to the experiment. Electrical resistance/conductivity tests were conducted to determine how cryogenic treatment affected the materials. The weight of the workpieces and tool electrodes was measured using a computerized weighing

scale with a minimum count of 0.001 g both before and after machining. The material removal rate was calculated using Eq. 1.

$$MRR = \left( \frac{W_1 - W_2}{c \times T} \right), \quad (1)$$

where  $W_1$  is the mass of the workpiece before machining, (g);  $W_2$  is the mass of the workpiece after machining, (g);  $\rho$  is the density of the workpiece, ( $\text{gm}/\text{cm}^3$ );  $T$  is the cycle time, (min).

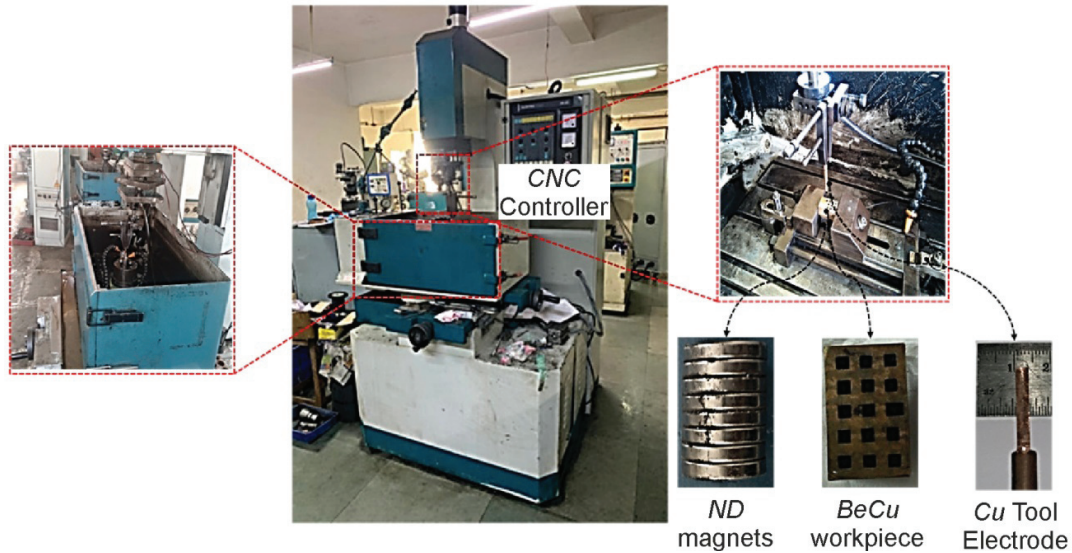


Fig. 1. Experimental set-up

The thickness of the white layer of each specimen was examined at  $850\times$  magnification using a scanning electron microscope. Next, the treated surfaces of the specimens were examined at  $1000\times$  magnification and surface cracks on the bottom and walls of the holes were measured. Using electrolytic copper tool electrodes, square holes with a depth of 5 mm from the surface were created on untreated *BeCu* alloy parts.

Figure 1 shows the experimental setup, which consisted of a *BeCu* workpiece, copper tool electrode, and magnets used for experimentation. A *BeCu* workpiece drilled with square holes with copper tool electrodes and magnets in the cutting zone. Experiments were carried out to understand the effect of cryogenic treatment of the workpiece and tool electrodes, along with the gap current and external magnetic strength, on the material removal rate. Thus, the experiments were carried out in two stages: a pilot study and main experiments based on the *Box-Behnken* design. To study the effects of the process parameters on the performance characteristics, the design variables are listed in Table 1.

Table 1

**Design variables**

Parameters	Performance measures
Gap current (A): 8, 10, 12, 14, 16	Material removal rate, white layer thickness, and crack length
Magnetic strength (T): 0, 0.124, 0.248, 0.372, 0.496	
Pulse on time: 38 $\mu\text{s}$	
Gap voltage: 55 V	
Pulse off time: 7 $\mu\text{s}$	
Dielectric: Commercial EDM oil	
Flushing pressure: 0.5 $\text{Kg}/\text{cm}^2$	
Polarity: Workpiece (-ve); Tool electrode (+ve)	

To make a decision on the range and level of gap current and magnetic field to obtain optimal values of material removal rate, pilot studies were carried out. The gap current and the gap current were varied at five levels; one pass was performed at each level. Various combinations of workpiece and tool were considered:

- *BeCu* (untreated) and *Cu* (untreated);
- *BeCu* (untreated) and *Cu* (cryogenically treated);
- *BeCu* (cryogenically treated) and *Cu* (untreated);
- *BeCu* (cryogenically treated) and *Cu* (cryogenically treated).

Based on the results obtained from the pilot study, the main experiments were designed using a three-variable *Box–Behnken* design.

## Results and Discussion

This section illustrates the *MRR* experimental results and its analysis, white layer thickness and crack formation and prediction of *MRR* using machine learning regressions.

### Experimental results and analysis

Experimental study was carried out in two phases. Firstly, one variable was varied over the selected levels at the fixed average values of the other variables. These experiments were conducted to study and normalize the *EDM* machine settings and process responses in general. It was determined that 5 mm was the proper depth of milling to achieve stability while the process was underway. Two variables were modified in this study: gap current and magnetic strength. The remaining variable was spread at equal intervals throughout its range, while the other variables were fixed at its respective average values for the whole range of options available in the machine. In the first five experiments, only the gap current was changed, as is illustrated in Table 2.

A similar variation was observed in the magnetic strength in five experiments as shown in Table 3. The gap current and magnetic strength varied for four workpiece and tool combinations.

Table 2

Experimental matrix: Varying gap current

Magnetic strength (T)	Gap voltage (V)	Gap current (A)	Pulse on time ( $\mu$ s)	Pulse off time ( $\mu$ s)	Workpiece and tool combinations ( <i>U:U</i> , <i>T:U</i> , <i>U:T</i> , and <i>T:T</i> )
0.248	55	8	38	7	<i>U:U</i> ( <i>BeCu</i> -untreated with <i>Cu</i> -untreated), <i>T:U</i> ( <i>BeCu</i> -treated with <i>Cu</i> -untreated), <i>U:T</i> ( <i>BeCu</i> -untreated with <i>Cu</i> -treated), <i>T:T</i> ( <i>BeCu</i> -treated with <i>Cu</i> -untreated)
0.248	55	10	38	7	
0.248	55	12	38	7	
0.248	55	14	38	7	
0.248	55	16	38	7	

Table 3

Experimental matrix: Varying magnetic strength

Magnetic strength (T)	Gap voltage (V)	Gap current (A)	Pulse on time ( $\mu$ s)	Pulse off time ( $\mu$ s)	Workpiece and tool combinations ( <i>U:U</i> , <i>T:U</i> , <i>U:T</i> , and <i>T:T</i> )
0	55	12	38	7	<i>U:U</i> ( <i>BeCu</i> -untreated with <i>Cu</i> -untreated), <i>T:U</i> ( <i>BeCu</i> -treated with <i>Cu</i> -untreated), <i>U:T</i> ( <i>BeCu</i> -untreated with <i>Cu</i> -treated), <i>T:T</i> ( <i>BeCu</i> -treated with <i>Cu</i> -untreated)
0.124	55	12	38	7	
0.248	55	12	38	7	
0.372	55	12	38	7	
0.496	55	12	38	7	

In this study, only the gap current and external magnetic field was varied. It is known that the most influential parameter for the maximum *MRR* is the spark energy. During cryogenic treatment, the thermal vibration of atoms in metals decreases due to the temperature decrease. This results in a decrease in electrical resistivity and improved electrical conductivity. Owing to the cryogenic process, the homogeneity of the crystal structure increases, and the gaps and dislocations are dissolved, which improves the structural compactness and electrical conductivity. According to the *Wiedmann-Franz-Lorenz* law, an increase in electrical conductivity would increase thermal conductivity.

Figure 2 depicts *MRR* varying with gap current for treated and untreated *BeCu* alloys with treated and untreated copper tool electrodes (four workpiece and tool combinations – *U:U*, *T:U*, *U:T*, and *T:T*). The surface temperature of the workpiece tends to increase as a result of the increase in spark energy caused by the gap current. The substance melts as a result, and the molten metal is subsequently flushed away by the dielectric fluid. Due to the increased electrical conductivity of the workpiece after cryogenic treatment, the *MRR* increases. Debris from the undesired material removed from the workpiece is created in the machining zone during the *EDM* process. The machining efficiency is decreased because arcing occurs instead of sparking if it is not removed from the cutting zone.

Debris removal from the cutting zone is facilitated by the strength of the external magnetic field. Additionally, this keeps the particles in the cutting zone from clogging. As a result, the stability of the *EDM* process is improved. Figure 3 depicts *MRR* varying with magnetic field strength for treated and untreated *BeCu* alloys with treated and untreated copper tool electrodes (four workpiece and tool combinations – *U:U*, *T:U*, *U:T*, and *T:T*). With an increase in the gap current, the spark energy increases, increasing the surface temperature of the workpiece, thereby melting and evaporating material from the workpiece surface and increasing *MRR*.

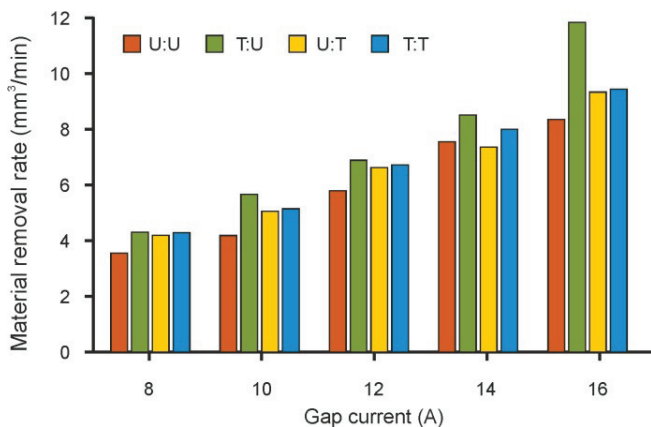


Fig. 2. *MRR* varying with gap current for four workpiece and tool combinations

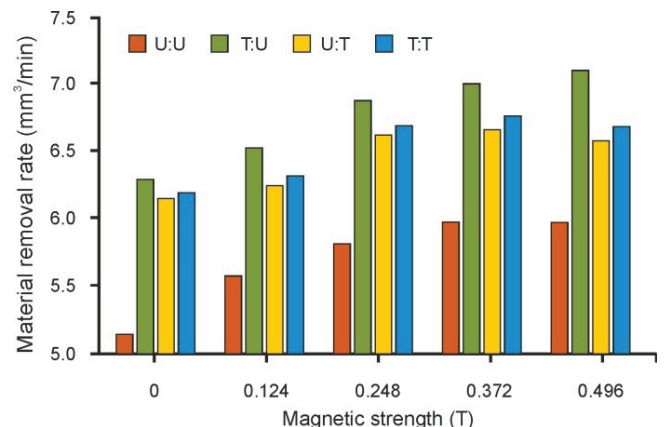


Fig. 3. *MRR* varying with magnetic strength for four workpiece and tool combinations

To understand the effect of input variables, namely the gap current ( $I_g$ ), external magnetic field strength ( $B$ ), and pulse-on time ( $T_{on}$ ), on the material removal rate (*MRR*) was investigated for cryogenically treated *BeCu* workpiece and untreated *Cu* electrode combination. This combination of workpiece and the tool is selected as it provided higher *MRR* among the other combinations of workpiece and the tool selected in the present study. Table 4 depicts the experimental matrix with *MRR* varying with  $I_g$ ,  $B$ , and  $T_{on}$ .

Experimentally based mathematical model (Eq. 2) was developed for the *MRR* for the *T:U* (*BeCu*-treated with *Cu*-untreated), workpiece and tool combination, for better understanding the *EDM* performance. The values of the coefficients involved in the equation were calculated using the *Microsoft Advanced Excel* data analysis tool.  $R$ -squared ( $R^2$ ) values which measure variation proportion in the data points are close to 0.912. Therefore, the developed model is reliable to predict the *MRR* during *EDM* of cryogenically treated *BeCu* workpiece with untreated *Cu* electrode.

$$MRR = 0.004501(I_g)^{1.339}(B)^{0.00121}(T_{on})^{1.0508} \quad (2)$$

Box–Behnken Design with observed values of *MRR*

Exp. No.	Gap current ( <i>I<sub>g</sub></i> ) (A)	Magnetic field ( <i>B</i> ) (T)	Pulse on time ( <i>T<sub>on</sub></i> ) (μs)	<i>MRR</i> (mm <sup>3</sup> /min)
1	8	NO	26	2.32
2	8	0.496	26	2.22
3	16	NO	26	6.00
4	16	0.496	26	6.54
5	12	NO	13	1.93
6	12	0.496	13	2.04
7	12	NO	38	4.66
8	12	0.496	38	5.003
9	8	0.248	13	0.97
10	16	0.248	13	1.88
11	8	0.248	38	2.89
12	16	0.248	38	7.40
13	12	0.248	26	4.86
14	12	0.248	26	4.64
15	12	0.248	26	4.78

Further, to have a better understanding of the effect of process parameters, *MRR* (figure 4) is plotted using the developed model varying with process parameters for the *T:U* (*BeCu*-treated with *Cu*-untreated), workpiece and tool combination. Figure 4, *a* depicts *MRR* varying with gap current at magnetic strength and pulse on time of 0.248 T and 26 s. The *MRR* can be seen as increasing with the gap current.

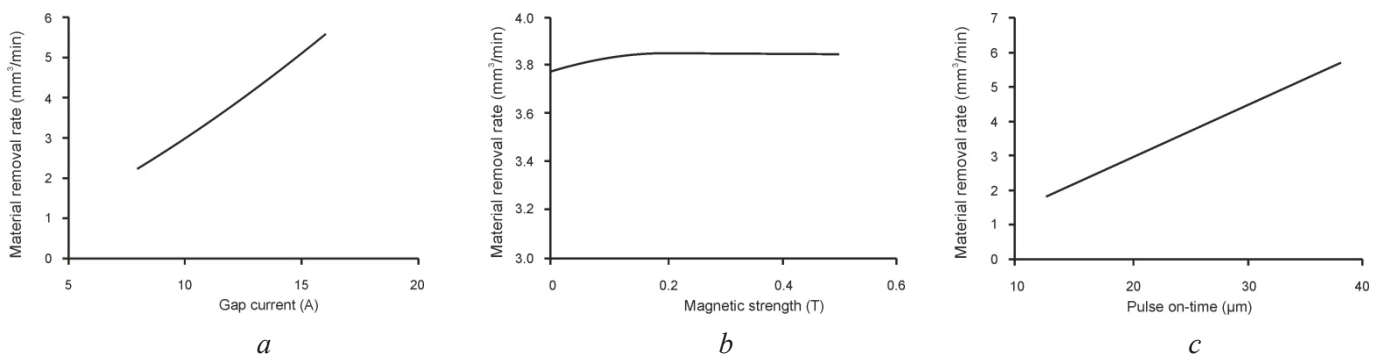


Fig. 4. *MRR* varying with Gap current (*a*), Magnetic field (*b*), and Pulse on time (*c*)

The *MRR* that changes with magnetic field at a gap current of 12 A and a pulse on time of 26 s is shown in figure 4, *b*. Furthermore, *MRR* fluctuates with pulse on time at gap current and magnetic strength of 12 A and 0.248 T, as shown in figure 4 *c*. A slight increase in *MMR* is observed with increasing magnetic strength. However, as demonstrated in figure 4, the *MRR* seems to increase with the pulse on time. The gap current has the biggest impact on the *MRR*, followed by the timing of the pulse and the magnetic field strength, which has a negligible effect.

According to figure 4, *MRR* values decrease with decreasing magnetic field and gap current values. As the values of gap current and magnetic field increase, the *MRR* also increases. With a magnetic field of 0.4 T and a gap current of 16 A, the *MMR* exceeds 7 mm<sup>3</sup>/min. Lower magnetic field and pulse on time values result in lower *MRR* readings. *MRR* increases simultaneously with an increase in magnetic field and pulse on time values. *MRR* exceeds 7 mm<sup>3</sup>/min with a magnetic field of 0.4 T and a pulse on time of 35 μs.

*MRR* values are lower for lower gap current and pulse on time values. As the gap current and pulse on time increase, the *MMR* also increases. With a current in the interelectrode gap of 16 A and a pulse interval of 35  $\mu\text{s}$ , the *SMR* exceeds 7  $\text{mm}^3/\text{min}$ . With a gap current of 16 A, a magnetic induction of 0.4709 T and a pulse of 38  $\mu\text{s}$ , the optimizer, using the principle of complex desirability, timely predicted the *MRR* value of 7.6453  $\text{mm}^3/\text{min}$ .

### White layer thickness (WLT)

As for the primary tests, the conditions that provided the highest rate of material removal were selected to test the white layer thickness (*WLT*). The thickness of the white layer is shown on the two separate edges of the square holes in figure 5, *a* and *b* for gap current of 8 A, magnetic strength of 0.248 T, gap voltage of 55 V, pulse on time of 13  $\mu\text{s}$  and pulse off time of 7  $\mu\text{s}$ .

Figure 5 shows that the low spark energy at 8 A gap current and 13  $\mu\text{s}$  pulse on duration resulted in limited white layer formation. It should be noted that the workpiece has a very low carbon content, which means that a white layer of less thickness is formed.

Figure 6, *a* and *b* illustrate the thickness of the white layer at two distinct corners of the square hole when the gap voltage is 55 V, the gap current is 8 A, the magnetic strength is 0.248 T, the pulse-on time is 38  $\mu\text{s}$ , and the pulse-off time is 7  $\mu\text{s}$ . Because of the higher spark energy in this trial circumstance compared to the prior case, there is a greater thickness of the white layer.

The white layer thickness at two separate square hole edges is depicted in figure 7, *a* and *b* with gap currents of 16 A, magnetic strengths of 0.248 T, gap voltages of 55 V, pulse on time of 38  $\mu\text{s}$ , and pulse off times of 7  $\mu\text{s}$ . In this scenario, the processing conditions are higher: the pulse on time is 38  $\mu\text{s}$  and the gap

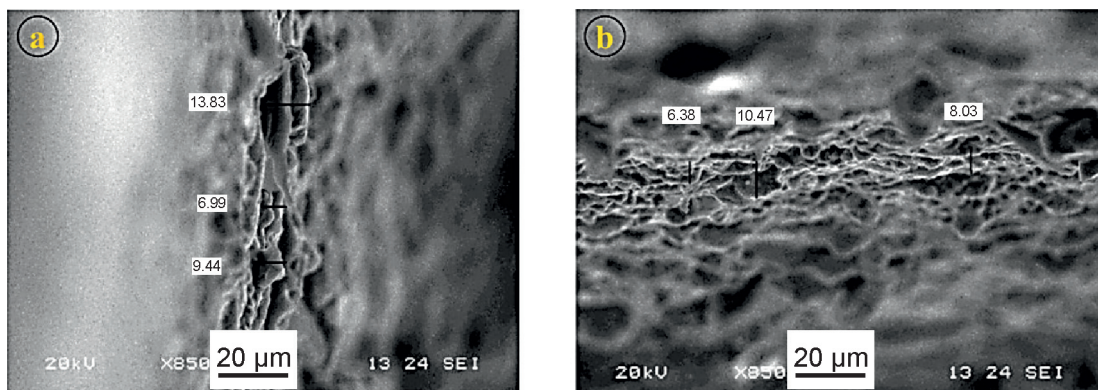


Fig. 5. WLT for Expt. 9 (Table 4) at the vertical cross-section of a square hole (*a*), at the horizontal cross-section of the square hole (*b*)

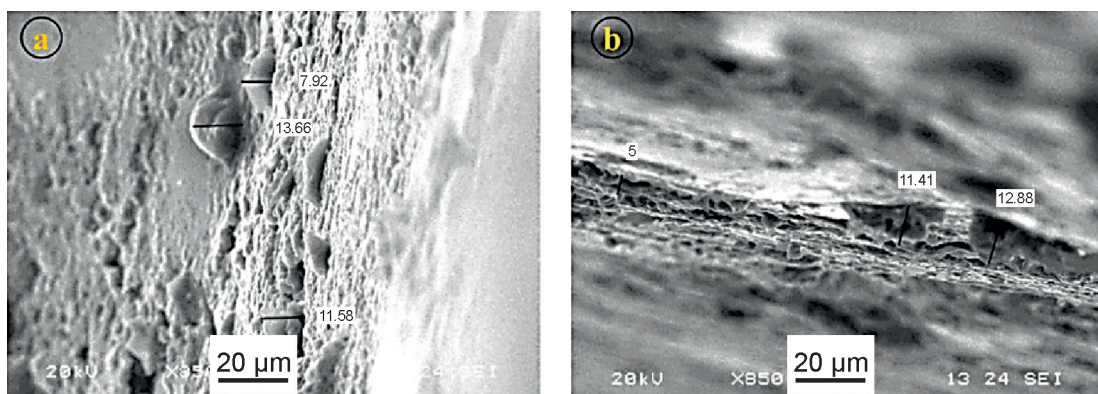


Fig. 6. WLT for Expt. 14 (Table 4) at the vertical cross-section of a square hole (*a*), the horizontal cross-section of the square hole (*b*)

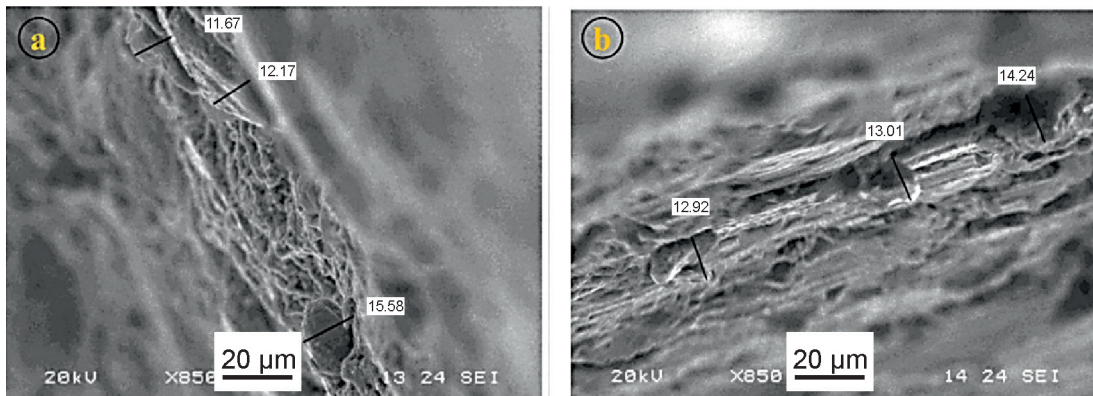


Fig. 7. WLT for Expt. 12 (Table 4) at the vertical cross-section of a square hole (a), the horizontal cross-section of the square hole (b)

current is 16 A. Thus, the white layer in this case is thicker than in the first two. However, the thickness of the white layer is typically less than 20  $\mu\text{m}$ , indicating that molten metal is effectively removed from the workpiece surface by dielectric flushing.

The white layer refers to a thin layer of recast material that forms on the surface of the workpiece after the electrical discharge process. This layer has different physical and chemical properties compared to the base material. The thickness of the white layer depends on various factors, including the *EDM* process parameters and the material being machined. Higher discharge energy increases material removal, resulting in a thicker white layer. Longer pulses provide greater energy transfer and may result in the formation of a thicker white layer. *BeCu* alloy has specific thermal and electrical conductivity properties that can affect the white layer formation. The composition and microstructure of the alloy can also play a role. Proper flushing of the machining zone helps remove debris and control the heat generated during the process, which can influence the white layer formation.

The observed white layer thickness at a low material removal rate for the horizontal surface is a minimum of 6.38  $\mu\text{m}$  and a maximum of 10.47  $\mu\text{m}$ . Similarly, for the vertical surfaces, the maximum and minimum are found to be 13.83  $\mu\text{m}$  and 6.99  $\mu\text{m}$ , respectively. The observed white layer thickness at a high material removal rate on the horizontal surface is at least 12.92  $\mu\text{m}$  and a maximum of 14.24  $\mu\text{m}$ . Similarly, for the vertical surface, the maximum and minimum are found to be 15.58  $\mu\text{m}$  and 11.67  $\mu\text{m}$ , respectively.

### *Crack formed on the machined surface*

The *EDM* process involves the generation of high temperatures on the workpiece surface. Rapid heating and subsequent cooling cycles can induce thermal stresses. These thermal stresses can lead to crack formation. Adequate cooling and flushing of the machining zone are crucial in *EDM* to control the temperature and remove debris. Insufficient flow or cooling of the dielectric fluid can result in excessive heating and thermal stress, increasing the likelihood of crack formation. Figure 8, *a* and *b* and figure 9? *a–d* show the crack and recast layer on the machined surface of the workpiece.

The cut section of the workpiece was examined using scanning electron microscopy. Photographs were taken of the bottom surface of the workpiece and the wall surface (figure 9 *e, f*). The specimen has very few surface cracks at low, medium and high material removal rates because the workpiece has superior thermal properties and a thinner white layer is formed on the surface. Cryogenic treatment of the workpiece and external magnetic strength prevented the formation of surface cracks and the formation of white layers.

## Conclusions

In the current study, the material removal rate, white layer thickness, and crack formation on the walls and bottom surface of a square hole produced by electrical discharge machining (*EDM*) were investigated by considering the effects of cryogenically machined combinations of copper-beryllium (*BeCu*) workpieces

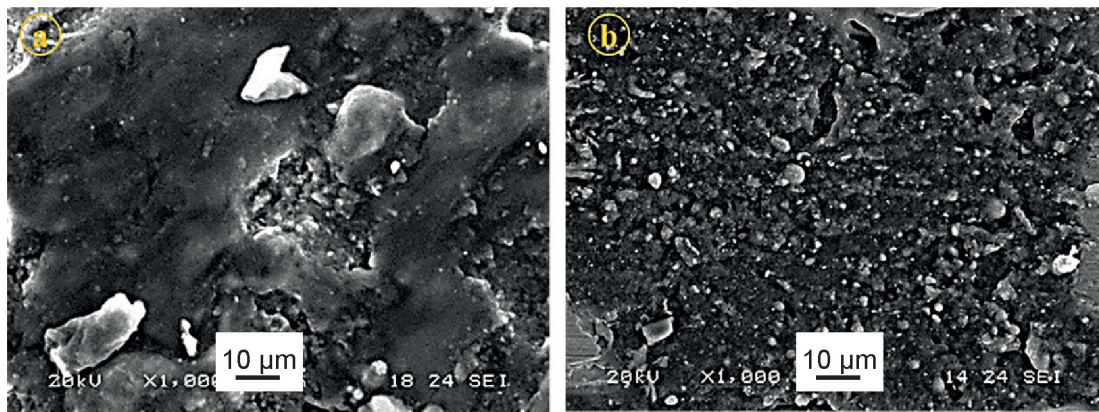


Fig. 8. Cracks for Expt. 9 at the wall surface of square hole (a); at the bottom surface of square hole (b)

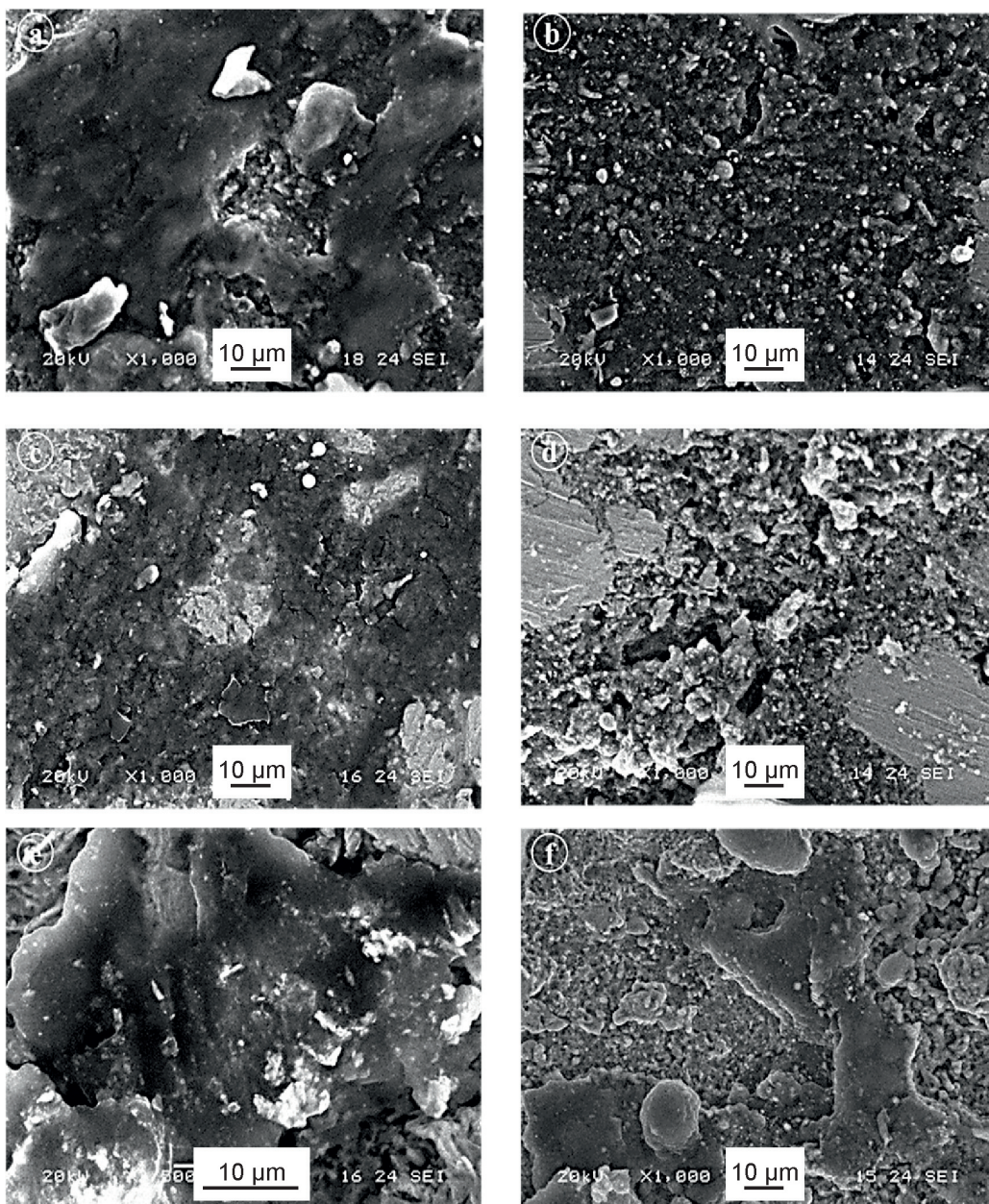


Fig. 9. Cracks at the wall surface of square hole for Expt. 14 (a); at the bottom surface of square hole for Expt. 14 (b); at the wall surface of square hole for Expt. 12 (c); at the bottom surface of square hole for Expt. 12 (d)



and copper (*Cu*) electrodes. Experiments were carried out with varying the gap current, magnetic field strength, and pulse on time. The pulse turn off time of 7  $\mu\text{s}$  and the gap voltage of 55 V were kept constant for all experiments. The thickness of the white layer and the formation of surface cracks were also investigated as a function of the *EDM* process parameters. To determine the final process input parameter levels for the primary experiments, a pilot study was first conducted. Second, the *Box-Behnken* design of experiments was followed in the planning and execution of the primary studies. Based on the experiments, a mathematical model was created to predict and maximize *MRR* by optimizing *EDM* performance. This study allows us to draw the following conclusions.

- The cryogenically treated *BeCu* workpiece and untreated *Cu* electrode combination provided higher *MRR* among the other combinations of workpiece and the tool selected in the present study.
- The gap current had the biggest impact on the *MRR*, followed by the timely pulse and the magnetic field strength, which had a negligible effect. The *MRR* was a minimum of 0.9  $\text{mm}^3/\text{min}$  and a maximum of 11.807  $\text{mm}^3/\text{min}$ .
- The observed white layer thickness at a low material removal rate for the horizontal surface was a minimum of 6.38  $\mu\text{m}$  and a maximum of 10.47  $\mu\text{m}$ . Similarly, for the vertical surfaces, the maximum and minimum were 13.83  $\mu\text{m}$  and 6.99  $\mu\text{m}$ , respectively.
- The observed white layer thickness at a high material removal rate on the horizontal surface was a minimum of 12.92  $\mu\text{m}$  and a maximum of 14.24  $\mu\text{m}$ . Similarly, for the vertical surface, the maximum and minimum were 15.58  $\mu\text{m}$  and 11.67  $\mu\text{m}$ , respectively.
- *SEM* images were obtained on the wall and bottom surfaces of the workpiece. Negligible surface cracks were observed for low, medium, and high material removal rates.
- It is evident that, owing to the cryogenic treatment of the workpiece and external magnetic strength, the white layer formation and surface crack formation were low.

## References

1. Vora J., Khanna S., Chaudhari R., Patel V.K., Paneliya S., Pimenov D.Y., Giasin K., Prakash C. Machining parameter optimization and experimental investigations of nano-graphene mixed electrical discharge machining of nitinol shape memory alloy. *Journal of Materials Research and Technology*, 2022, vol. 19, pp. 653–668. DOI: 10.1016/j.jmrt.2022.05.076.
2. Akıncıoğlu S. Taguchi optimization of multiple performance characteristics in the electrical discharge machining of the TiGr2. *Facta Universitatis. Series: Mechanical Engineering*, 2022, vol. 20 (2), pp. 237–253. DOI: 10.22190/FUME201230028A.
3. Danish M., Al-Amin M., Abdul-Rani A.M., Rubaiee S., Ahmed A., Zohura F.T., Ahmed R., Yildirim M.B. Optimization of hydroxyapatite powder mixed electric discharge machining process to improve modified surface features of 316L stainless steel. *Proceedings of the Institution of Mechanical Engineers, Part E: Journal of Process Mechanical Engineering*, 2023, vol. 237 (3), pp. 881–895. DOI: 10.1177/09544089221111584.
4. Kam M., İpekçi A., Argun K. Experimental investigation and optimization of machining parameters of deep cryogenically treated and tempered steels in electrical discharge machining process. *Proceedings of the Institution of Mechanical Engineers, Part E: Journal of Process Mechanical Engineering*, 2022, vol. 236 (5), pp. 1927–1935. DOI: 10.1177/09544089221078133.
5. Gautam N., Goyal A., Sharma S.S., Oza A.D., Kumar R. Study of various optimization techniques for electric discharge machining and electrochemical machining processes. *Materials Today: Proceedings*, 2022, vol. 57, pp. 615–621. DOI: 10.1016/j.matpr.2022.02.005.
6. Shukla S.K., Priyadarshini A. Application of machine learning techniques for multi objective optimization of response variables in wire cut electro discharge machining operation. *Materials Science Forum*, 2019, vol. 969, pp. 800–806. DOI: 10.4028/www.scientific.net/MSF.969.800.
7. Kumar Vin., Kumar Vik., Jangra K.K. An experimental analysis and optimization of machining rate and surface characteristics in WEDM of Monel-400 using RSM and desirability approach. *Journal of Industrial Engineering International*, 2015, vol. 11 (3), pp. 297–307. DOI: 10.1007/s40092-015-0103-0.
8. Kumar S.V., Kumar M.P. Optimization of cryogenic cooled EDM process parameters using grey relational analysis. *Journal of Mechanical Science and Technology*, 2014, vol. 28, pp. 3777–3784. DOI: 10.1007/s12206-014-0840-9.



9. Gangele A., Mishra A. Surface roughness optimization during machining of niti shape memory alloy by EDM through Taguchi's technique. *Materials Today: Proceedings*, 2020, vol. 29, pp. 343–347. DOI: 10.1016/j.matpr.2020.07.287.
10. Ghosh I., Sanyal M., Jana R., Dan P.K. Machine learning for predictive modeling in management of operations of EDM equipment product. *2016 Second International Conference on Research in Computational Intelligence and Communication Networks (ICRCICN)*. IEEE, 2016, pp. 169–174. DOI: 10.1109/ICRCICN.2016.7813651.
11. Ulas M., Aydur O., Gurgenc T., Ozel C. Surface roughness prediction of machined aluminum alloy with wire electrical discharge machining by different machine learning algorithms. *Journal of Materials Research and Technology*, 2020, vol. 9 (6), pp. 12512–12524. DOI: 10.1016/j.jmrt.2020.08.098.
12. Kumar N.A., Babu A.S. Influence of input parameters on the near-dry WEDM of Monel alloy. *Materials and Manufacturing Processes*, 2018, vol. 33 (1), pp. 85–92. DOI: 10.1080/10426914.2017.1279297.
13. Pogrebnyak A., Bratushka S., Beresnev V.M., Levintant-Zayonts N. Shape memory effect and superelasticity of titanium nickelide alloys implanted with high ion doses. *Russian Chemical Reviews*, 2013, vol. 82 (12), p. 1135. DOI: 10.1070/RC2013v082n12ABEH004344.
14. Ming W., Zhang S., Zhang G., Du J., Ma J., He W., Cao C., Liu K. Progress in modeling of electrical discharge machining process. *International Journal of Heat and Mass Transfer*, 2022, vol. 187, p. 122563. DOI: 10.1016/j.ijheatmasstransfer.2022.122563.
15. Shastri R.K., Mohanty C.P., Dash S., Gopal K.M.P., Annamalai A.R., Jen C.P. Reviewing performance measures of the die-sinking electrical discharge machining process: challenges and future scopes. *Nanomaterials*, 2022, vol. 12 (3), p. 384. DOI: 10.3390/nano12030384.
16. Boopathi S. An extensive review on sustainable developments of dry and near-dry electrical discharge machining processes. *Journal of Manufacturing Science and Engineering*, 2022, vol. 144 (5), p. 050801. DOI: 10.1115/1.4052527.
17. Ali M.A., Samsul M., Hussein N.I., Rizal M., Izamshah R., Hadzley M., Kasim M.S., Sulaiman M.A., Sivarao S. The effect of EDM die-sinking parameters on material removal rate of beryllium copper using full factorial method. *Middle-East Journal of Scientific Research*, 2013, vol. 16 (1), pp. 44–50. DOI: 10.5829/idosi.mejsr.2013.16.01.2249.
18. Daneshmand S., Kahrizi E.F., Abedi E., Abdolhosseini M.M. Influence of machining parameters on electro discharge machining of NiTi shape memory alloys. *International Journal of Electrochemical Science*, 2013, vol. 8 (3), pp. 3095–3104. DOI: 10.1016/S1452-3981(23)14376-8.
19. Daneshmand S., Monfared V., Lotfi Neyestanak A.A. Effect of tool rotational and Al<sub>2</sub>O<sub>3</sub> powder in electro discharge machining characteristics of NiTi-60 shape memory alloy. *Silicon*, 2017, vol. 9 (2), pp. 273–283. DOI: 10.1007/s12633-016-9412-1.
20. Baroi B.K., Jagadish, Patowari P.K. A review on sustainability, health, and safety issues of electrical discharge machining. *Journal of the Brazilian Society of Mechanical Sciences and Engineering*, 2022, vol. 44 (2), p. 59. DOI: 10.1007/s40430-021-03351-4.
21. Kannan E., Trabelsi Y., Boopathi S., Alagesan S. Influences of cryogenically treated work material on near-dry wire-cut electrical discharge machining process. *Surface Topography: Metrology and Properties*, 2022, vol. 10 (1), p. 015027. DOI: 10.1088/2051-672X/ac53e1.
22. Abdulkareem S., Khan A.A., Konneh M. Reducing electrode wear ratio using cryogenic cooling during electrical discharge machining. *The International Journal of Advanced Manufacturing Technology*, 2009, vol. 45, pp. 1146–1151. DOI: 10.1007/s00170-009-2060-5.
23. Gill S.S., Singh J. Effect of deep cryogenic treatment on machinability of titanium alloy (Ti-6246) in electric discharge drilling. *Materials and Manufacturing Processes*, 2010, vol. 25 (6), pp. 378–385. DOI: 10.1080/10426910903179914.
24. Srivastava V., Pandey P.M. Performance evaluation of electrical discharge machining (EDM) process using cryogenically cooled electrode. *Materials and Manufacturing Processes*, 2012, vol. 27 (6), pp. 683–688. DOI: 10.1080/10426914.2011.602790.
25. Yildiz Y., Sundaram M., Rajurkar K., Nalbant M. The effects of cold and cryogenic treatments on the machinability of beryllium-copper alloy in electro discharge machining. *44th CIRP Conference on Manufacturing Systems*, Madison, Wisconsin, 2011, pp. 1–6.
26. Singh R., Singh B. Comparison of cryo-treatment effect on machining characteristics of titanium in electric discharge machining. *International Journal of Automotive and Mechanical Engineering*, 2011, vol. 3, pp. 239–248. DOI: 10.15282/ijame.3.2011.1.0020.



27. Nadig D., Ramakrishnan V., Sampathkumaran P., Prashanth C. Effect of cryogenic treatment on thermal conductivity properties of copper. *AIP Conference Proceedings*, 2012, vol. 1435 (1), pp. 133–139.
28. Srivastava V., Pandey P.M. Effect of process parameters on the performance of EDM process with ultrasonic assisted cryogenically cooled electrode. *Journal of Manufacturing Processes*, 2012, vol. 14 (3), pp. 393–402. DOI: 10.1016/j.jmapro.2012.05.001.
29. Liqing L., Yingjie S. Study of dry EDM with oxygen-mixed and cryogenic cooling approaches. *Procedia CIRP*, 2013, vol. 6, pp. 344–350.
30. Jafferson J., Hariharan P. Machining performance of cryogenically treated electrodes in microelectric discharge machining: a comparative experimental study. *Materials and Manufacturing Processes*, 2013, vol. 28 (4), pp. 397–402.
31. Mathai V., Vaghela R., Dave H., Raval H., Desai K. Study of the effect of cryogenic treatment of tool electrodes during electro discharge machining. *Proceedings of the Eighth International Conference on Precision Meso, Micro & Nano Engineering (COPEN-8: 2013)*, National Institute of Technology, Calicut, India, 2013, pp. 13–15.
32. Singh J., Singh G., Pandey P.M. Electric discharge machining using rapid manufactured complex shape copper electrode with cryogenic cooling channel. *Proceedings of the Institution of Mechanical Engineers, Part B: Journal of Engineering Manufacture*, 2021, vol. 235 (1–2), pp. 173–185. DOI: 10.1177/0954405420949102.
33. Prakash D., Tariq M., Davis R., Singh A., Debnath K. Influence of cryogenic treatment on the performance of micro-EDM tool electrode in machining of magnesium alloy AZ31B. *Materials Today: Proceedings*, 2021, vol. 39, pp. 1198–1201. DOI: 10.1016/j.matpr.2020.03.589.
34. Karthik Pandiyan G., Prabakaran T., Jafrey Daniel James D., Sivalingam V. Machinability analysis and optimization of electrical discharge machining in AA6061-T6/15wt.% SiC composite by the multi-criteria decision-making approach. *Journal of Materials Engineering and Performance*, 2022, vol. 31 (5), pp. 3741–3752. DOI: 10.1007/s11665-021-06511-8.
35. Sawant D.A., Jatti V.S., Mishra A., Sefene E.M., Jatti A.V. Surface roughness and surface crack length prediction using supervised machine learning-based approach of electrical discharge machining of deep cryogenically treated NiTi, NiCu, and BeCu alloys. *International Journal of Advanced Manufacturing Technology*, 2023, vol. 128, pp. 5595–5612. DOI: 10.1007/s00170-023-12269-1.

## Conflicts of Interest

The authors declare no conflict of interest.

© 2024 The Authors. Published by Novosibirsk State Technical University. This is an open access article under the CC BY license (<http://creativecommons.org/licenses/by/4.0>).

